IEEE *Access*

Design of a Frequency and Polarization Reconfigurable Patch Antenna With a Stable Gain

JUN HU[ID], (Student Member, IEEE), AND ZHANG-CHENG HAO[ID], (Senior Member, IEEE)

State Key Laboratory of Millimeter Waves, Southeast University, Nanjing 210096, China

Corresponding author: Zhang-Cheng Hao (zchao@seu.edu.cn)

ABSTRACT This paper presents a frequency and polarization reconfigurable patch antenna with a small gain variation. Eight discrete operating frequency bands can be achieved by properly switching shorting pins, and three polarization states, i.e., left-hand circularly polarization, right-hand circularly polarization, and linearly polarization, can be realized simultaneously by adjusting perturbation segments. A stable gain performance is obtained within a wide reconfigurable frequency range, as well as all the reconfigurable polarization states, by utilizing the loss-character of p-i-n diodes when shorting pins are properly switched ON/OFF for different states. A prototype is designed, fabricated, and measured. The simulated and measured results agree as well. The experimental results show that the proposed antenna exhibits a simple reconfigurable network, a wide switching frequency range, a good element gain, and a small gain variation less than 1.8 dB across all the operating states.

INDEX TERMS Patch antenna, polarization reconfigurable, frequency reconfigurable, agile antenna.

I. INTRODUCTION

With the rapid development of modern wireless communication systems, the research on reconfigurable antennas has been a hot topic due to their ability to provide multiple functionalities. Typically, the adjustable parameters are operating frequency, pattern and polarization [1]–[36]. In the past decade, many reconfigurable antennas with a single tunable parameter have been developed and applied for wireless communications. For example, frequency reconfigurable antennas are developed in [1]–[3], pattern reconfigurable antennas are reported in [4]–[12], and polarization reconfigurable antennas are investigated in [13]–[21]. All those antennas exhibit good performance in terms of single reconfigurable character such as frequency, pattern or polarization.

As the working environment becomes more and more complex, reconfigurable antennas are strongly expected to have the ability to alter multi-parameters [22]–[36]. For example, multi-parameter reconfigurable antennas are attractive for the anti-jam or anti-intercept wireless system, which can improve significantly the system security. Reconfigurable antennas with frequency agility and polarization diversity have many advantages, such as efficient spectrum utilization, increased system capacity by polarization diversity, and

improved communication security by randomly selecting the operating modes. In an agile wireless system with multiple reconfigurable parameters, a stable gain for all the operating modes is highly expected, which is helpful to increase the system efficiency, reduce the system cost, and realize a good signal/noise ratio. Recently, a number of implementations with combined frequency and polarization reconfigurability [26]–[36] have been successfully developed by using varactor diodes, RF switches, such as p-i-n diodes and microelectromechanical systems (MEMS) switches, and other techniques. Although those antennas exhibit good reconfigurable performance of wide frequency range and multi polarization states, they usually face challenges including complicated reconfigurable feeding networks, larger gain variations among reconfigurable modes, or a small reconfigurable frequency range.

In this paper, a frequency and polarization reconfigurable patch antenna with a consistent gain has been proposed with more reconfigurable states and wider reconfigurable frequency bands by combing the switchable shorting pins and perturbation patches based on [36]. The switchable shorting pins are used to implement frequency agility, and the four controllable perturbation segments are for realizing

polarization diversity. Both the frequency and polarization of the proposed antenna can be independently switched among different operating states, including eight frequency bands and three polarization modes. In addition, by utilizing the loss-character of p-i-n diodes, the radiation efficiency of the proposed antenna has an opposite variation trend as that of directivity in a wide frequency range through the varied ohm losses from properly switched p-i-n diodes, and the detailed explanation is given in the Section III. As a result, a stable realized gain performance is obtained within a wide reconfigurable frequency range, as well as all the reconfigurable polarization states.

The rest of this paper is organized as follows. Section II shows the design and operational principle of the proposed antenna in detail. Then, a prototype is designed, fabricated and tested. Both the simulation and measurement results of the fabricated antenna for all the operating frequency bands and polarization modes are presented and discussed in Section III. Finally, conclusions are given in Section IV.

II. ANTENNA DESIGN AND OPERATION PRINCIPLE

The 3-D structure and geometrical configuration of the proposed antenna are shown in Fig. 1. The antenna is implemented on the Rogers 5880 ($\tan\delta = 0.0009$ at 10 GHz) substrate with a relatively permittivity of $\varepsilon_r = 2.2$ and a thickness of $H = 3.175$-mm. The antenna structure is composed of a square patch, three groups of switchable shorting pins connected to the ground plane, and four controllable perturbation segments connected to the corner of the square patch via p-i-n diode. The antenna is fed by a coaxial probe through a microstrip line. In order to obtain a better impedance match for LP mode, a stub with a length of L_2 is connected to the feeding line via a p-i-n diode. It should be mentioned that although a fixed polarization state such as the linear polarization or the circular polarization can be realized by only using properly designed shorting pins [37]–[40], multiple excitation ports have to be adopted if a switchable polarization performance is desired, and that leads to a complicated reconfigurable feeding network as well as matching circuits. To overcome this shortcoming, square perturbation segments with a width of W_2 are used to implement polarization reconfigurable, and the switchable shorting pins are for frequency agility in this work.

The whole antenna has been simulated and optimized by using the full-wave commercial software, i.e., the HFSS simulator, in which the p-i-n diode is modeled as a low resistance for ON state and open for OFF state. For reconfiguring polarization, four controllable perturbation segments are added and connected to the host patch via four p-i-n diodes ($D1$-$D4$). For switching these p-i-n diodes, the biasing voltage is supplied through a RF choke inductor and the biasing circuits are designed on the ground plane, which has a little effect on the antenna performance. When the two p-i-n diodes in the opposite direction ($D1\&D2$ or $D3\&D4$) are switched ON, the two orthogonal modes will be split in resonant frequency with equal amplitude and 90-degree phase-difference which
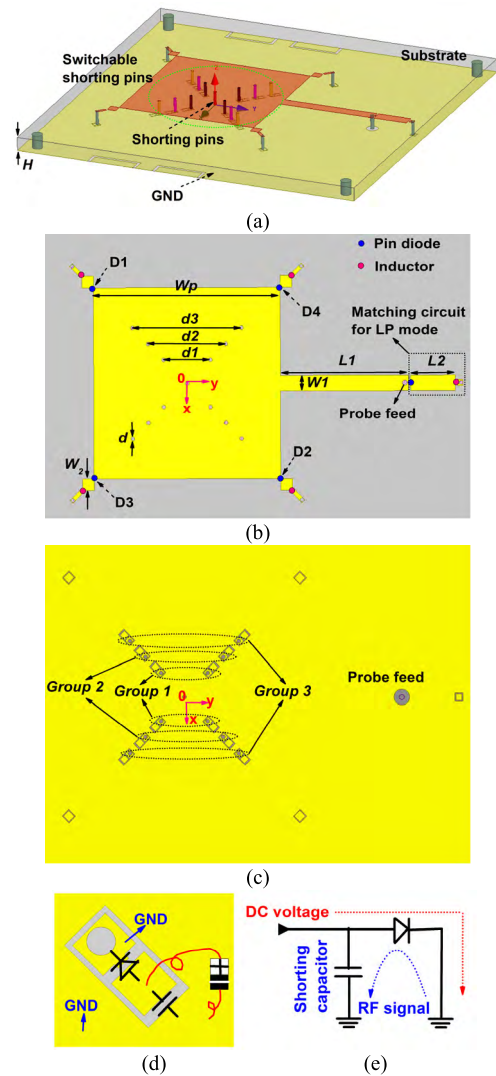
FIGURE 1. Geometrical configuration of the proposed frequency and polarization reconfigurable patch antenna. (a) 3-D structure. (b) top layer layout. (c) bottom layer layout. (d) biasing circuit for the switchable shorting pins. (e) equivalent circuit. (Unit: mm. $d = 1$, $d1$=12, $d2$=20, $d3$=28, $W1$=4, $W2$=3, Wp=48, $L1$=33, $L2$=12, H=3.175)

can produce a CP wave in the far-field region. When all the four p-i-n diodes are turned ON, the antenna has a symmetrical structure and radiates LP wave. In order to confirm the polarization diversity, the full-wave simulated 1.85 GHz vector surface current distributions on the patch for the three polarization modes are illustrated in Fig. 2. It can be clearly seen from Fig. 2 that the two orthogonal modes are excited with 90-degree phase-difference when the two p-i-n diodes in the opposite direction ($D1\&D2$ or$D3\&D4$) are switched ON. Hence, by controlling the states of $D1$-$D4$, the polarization of the antenna can be switched among three polarization states, i.e., LHCP, RHCP and LP. The relationships between the polarization and the states of $D1$-$D4$ are tabulated in Table 1.

The resonant frequency of the proposed antenna is switched by using twelve switchable shorting pins, which are divided into three groups, i.e., group 1-3, as labeled
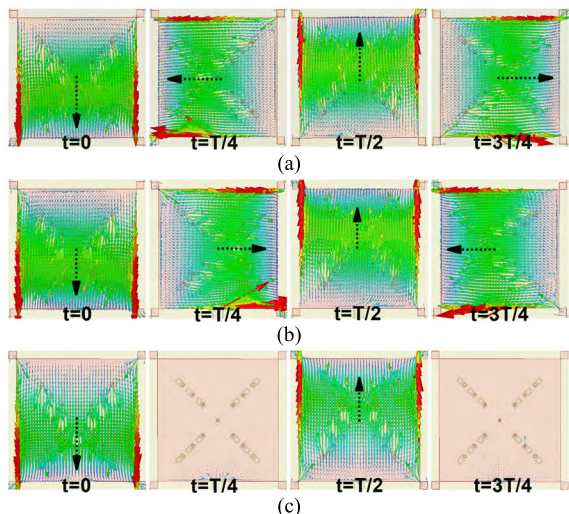
FIGURE 2. Simulated 1.85 GHz surface current distributions of the proposed antenna at four different time phases for the three polarization states. (a) LHCP. (b) RHCP. (c) LP.

TABLE 1. States of controllable perturbation segments for different polarization states.
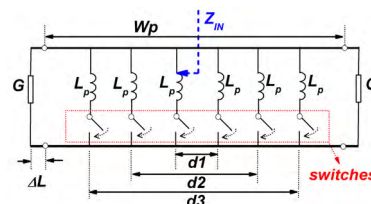
D1	D2	D3	D4	Polarization
ON	ON	OFF	OFF	LHCP
OFF	OFF	ON	ON	RHCP
ON	ON	ON	ON	LP

TABLE 2. States of switchable shorting pins for different operating frequency bands.

Group 1	Group 2	Group 3	Operating frequency band
OFF	OFF	OFF	Band 1
ON	OFF	OFF	Band 2
OFF	ON	OFF	Band 3
ON	ON	OFF	Band 4
OFF	OFF	ON	Band 5
ON	OFF	ON	Band 6
OFF	ON	ON	Band 7
ON	ON	ON	Band 8

FIGURE 3. The equivalent model of the proposed patch antenna with switchable shorting pins.

in Fig. 1(c). Each group has four switchable shorting pins that are placed in the two diagonals of the square patch, and the pin-to-pin spacing are denoted as d_1, d_2, d_3, respectively, as illustrated in Fig. 1. The diameter of all the shorting pins is d. P-i-n diodes are employed in the design of the switchable shorting pins. In order to reduce the effect on antenna performance, all the biasing circuits for switching these p-i-n diodes are designed on the ground plane, and the detail layout is shown in Fig. 1(d). The biasing voltage is supplied through a wire welded into the isolated area. In the biasing circuits, DC-blocking capacitors are used to connect the isolated area to the bottom ground plane. The equivalent circuit has been drawn in Fig. 1(e). The DC-blocking capacitors have low impedance in the operating frequency band and can be seen as shorting capacitor. So the effect from the biasing circuit can be reduced to acceptable levels. By switching the different states of these switchable shorting pins, the operating frequency band of the dominant mode in the patch antenna can be dynamically selected from eight discrete frequency bands, which are listed in Table 2.

The operating frequency agility mechanism of the patch antenna can be explained by using an equivalent transmission line model in Fig. 3, whose parameters can be initially obtained by the formulas in [37]. The resonant condition is that the imaginary part of the input impedance Z_{IN}, which is obtained by seeing from the middle to left or right as shown in Fig. 3, is equal to zero. It is clear that the position of the

shorting pins affects the input impedance. So the resonant frequency can be adjusted by tuning these shorting pins. When all the shorting pins are turned OFF, half the length of transmission line, i.e., $\Delta L + Wp/2$, $\Delta L + Wp$ is equal to one-quarter-wavelength at the resonant frequency. However, when the shorting pins are switched on, the resonant frequency goes up due to the shunt inductive effect of the shorting pins, which needs to be finely optimized by using the HFSS. By adjusting the number and distance of the shorting pins, the resonant frequency can be tuned over a relatively larger range of 1-1.5 [35].

In order to understand the operating principle more clearly from the physical point of view, the electric field vector distributions of the dominant mode with different shorting pins are plotted in Fig. 4. As shown in Fig. 4(a), when all the shorting pins are switched OFF, the electric field vector beneath the patch manifests a standard TM_{01} mode and it resonates at 1.85 GHz. If all the shorting pins are switched ON, the electric field is obviously removed outward, which indicates that the antenna resonates at a high frequency of 2.63 GHz.
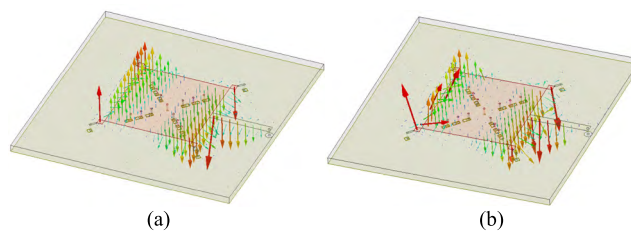
FIGURE 4. The electric field distribution of the proposed patch antenna with different shorting pins. (a) Switching all shorting pins OFF. (b) Switching all shorting pins ON.

III. RESULTS AND DISCUSSION

Based on the above analysis, an antenna prototype is designed, fabricated and measured. The photograph of the fabricated antenna is shown in Fig. 5. In the experiment, p-i-n diodes (MADP-000907-14020) [41] from MACOM are used as switches, and surface mount capacitors (860 pF) and inductor (22 nH) from Murata are adopted in the DC biasing circuits. The reflection coefficients for all the operating states are measured by the Agilent Vector Network Analyzer. The far-field performance is measured in a microwave chamber, and the fast rotating method is employed in the test for the CP modes. Hence, the AR performance can be extracted from the ripples of the radiation patterns [42], [43].
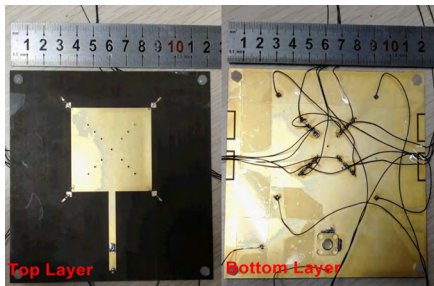

FIGURE 5. Photograph of the fabricated reconfigurable patch antenna.

The measured reflection coefficients, gains and AR properties at the boresight direction for the three polarization states are compared with the corresponding simulated results in Fig. 6-8. The measured results show a good agreement with the simulated ones except for a slight deviation to the low frequency, which is mainly resulted by the tolerance of the position of the shorting pins. The 3 dB AR bandwidth becomes wider as the operating frequency increases. This is due to the relatively larger electrically thickness of the substrate at the high frequency. The bandwidths for each operating state are narrow and can be increased by some techniques, such as increasing the thickness of the substrate, adding parasitic patch, employing stack structure and so on.
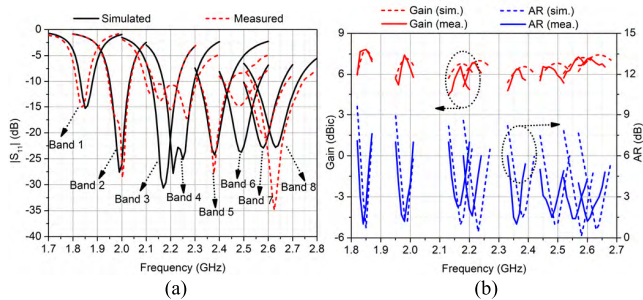

FIGURE 6. Measured and simulated results of the fabricated antenna at LHCP mode. (a) $|S_{11}|$. (b) gain and AR.

The measured peak gains at each operating frequency band for the three polarization states are plotted in Fig. 9(a). As shown in Fig. 9(a), the realized peak gains are larger than
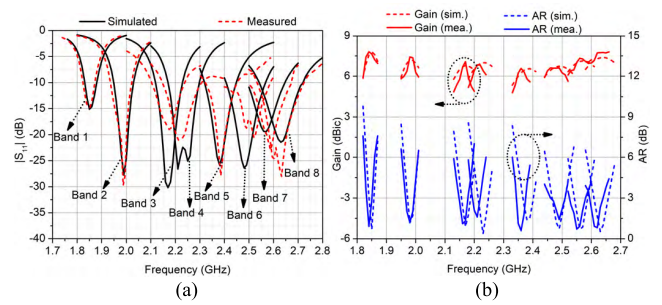

FIGURE 7. Measured and simulated results of the fabricated antenna at RHCP mode. (a) $|S_{11}|$. (b) gain and AR.
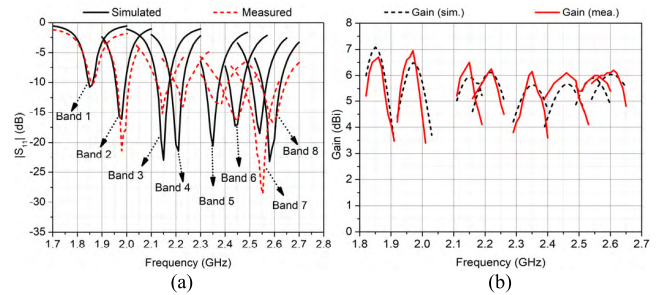

FIGURE 8. Measured and simulated results of the fabricated antenna at LP mode. (a) $|S_{11}|$. (b) gain.
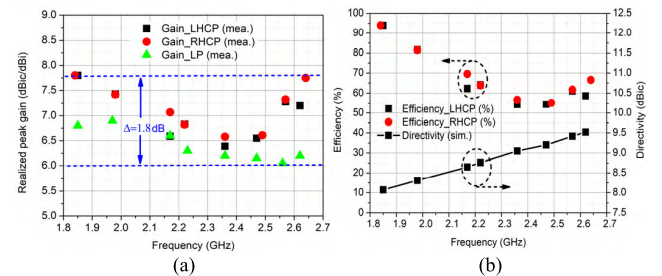

FIGURE 9. Measured peak gains and efficiency at all the operating frequency bands. (a) Realized peak gains. (b) Efficiency and directivity.

6 dBi/dBic. In addition, the peak gains variation across all the operating frequency bands and polarization modes is less than 1.8 dB. It is notably to mention here that the stable gain is an important advantage of the proposed frequency reconfigurable antenna over the referenced antennas, as shown in Table 3. The obtained constant gain over a wide frequency can be explained by combining with radiation efficiency. Fig. 9(b) presents the simulated directivity and the measured radiation efficiency, which is obtained by calculating the ratio of the measured gain to the simulated directivity, for the two CP modes. As shown in Fig. 9(b), the directivity of the patch antenna keeps increasing as the operating frequency goes up because of the larger antenna aperture at the high frequency. However, the variation tendency of the radiation efficiency is to decline firstly and then to rise a little at the high operating frequency, which is caused by different states of the switchable shorting pins. When the antenna

TABLE 3. Performance comparison with the existing state of art.

| Reference	Polarization Reconfiguration	Frequency range (GHz)	Peak Gain (dBi/dBic)	Gain fluctuation (dB)	Antenna Type	Efficiency (min.)	No. of switches
[26]	two LP two CP	continuous (1.5-2.4)	13.29	4.84	1×4 array	53%	4 varactor diodes, a polarization control feed network
[27]	one LP two CP	three operating frequency bands (1.67-1.91)	n. a.	n. a.	element	n. a.	2 varactor diodes, 2 p-i-n diodes
[28]	six LP	five discrete frequency bands	3.1	6.1	element	about 25%	a large number of p-i-n diodes
[29]	LHCP, RHCP	continuous (1.03-1.54)	n. a.	n. a.	element	n. a.	dual-polarized tunable EBG by a larger number of varactor diodes
[30]	full polarization	continuous (0.9-1.5)	3	larger than 12	element	lower than 5%	2 RF MEMS SPDT switches, 4 varactor diodes
[32]	three LP	continuous (1.35-2.25)	6.8	9.6	element	low	4 varactor diodes, 12 p-i-n diodes
[33]	two LP two CP	continuous (2.4-3.6)	9.6	7.6	element	25%	12 varactor diodes
This work	one LP two CP	eight operating frequency bands (1.83-2.65)	7.8	1.8	element	54%	16 p-i-n diodes
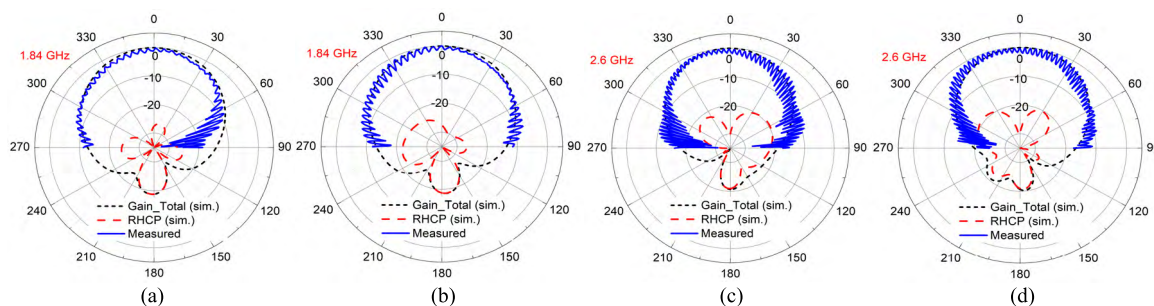
FIGURE 10. Measured and simulated normalized radiation patterns of the antenna at LHCP mode. (a) $\varphi = 0^0$ plane at 1.84 GHz. (b) $\varphi = 90^0$ plane at 1.84 GHz. (c) $\varphi = 0^0$ plane at 2.6 GHz. (d) $\varphi = 90^0$ plane at 2.6 GHz.

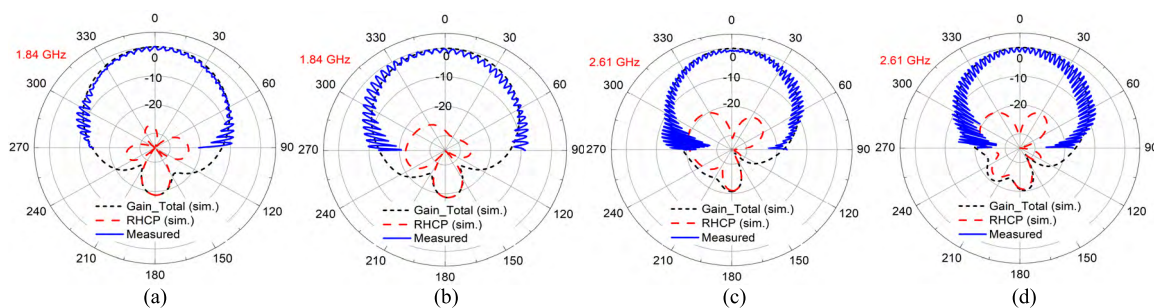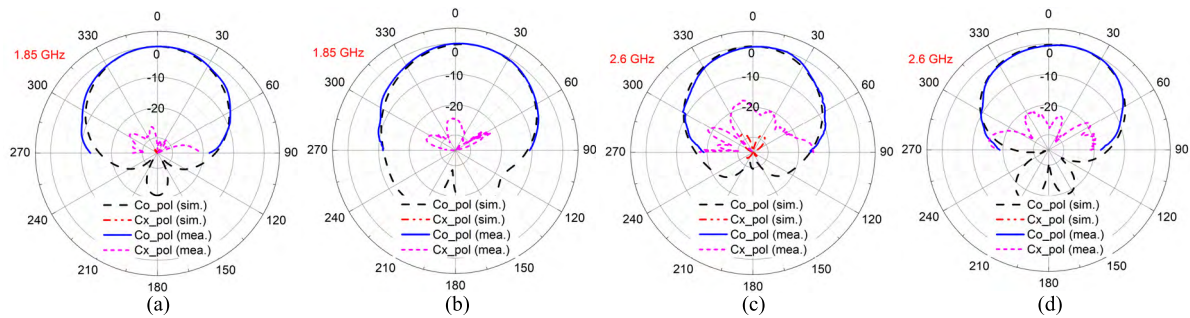**FIGURE 11.** Measured and simulated normalized radiation patterns of the antenna at RHCP mode. (a) $\varphi = 0^0$ plane at 1.84 GHz. (b) $\varphi = 90^0$ plane at 1.84 GHz. (c) $\varphi = 0^0$ plane at 2.61 GHz. (d) $\varphi = 90^0$ plane at 2.61 GHz.

operates at the band 1, all the shorting pins are switched OFF and no RF current passes through the corresponding p-i-n diodes. So the antenna operating at the band 1 has a high efficiency of 94%. As the working frequency goes up, the corresponding shorting pins are switched ON and RF current must pass through the p-i-n diodes when the p-i-n diodes can be modeled as a low resistor. Hence, the efficiency is deteriorated. Moreover, the outer shorting pins have a larger influence on the efficiency than the inner shorting pins. As the operating frequency increases further, more than one group of

shorting pins must be switched ON. In this case, the resistors that represent the p-i-n diodes switched ON are connected in parallel. So the total resistor gets smaller, which explicates that the efficiency rises a little at the high frequency. As a result, a peak gain with a little fluctuation less than 1.8 dB has been realized for all the operating states.

The measured and simulated normalized radiation patterns at the two orthogonal cut-planes are compared at two frequency points for the three polarizations modes, as shown in Fig. 10-12. Generally, the measured results are in good

FIGURE 12. Measured and simulated normalized radiation patterns of the antenna at LP mode. (a) H-plane at 1.85 GHz. (b) E-plane at 1.85 GHz. (c) H-plane at 2.6 GHz. (d) E-plane at 2.6 GHz.

agreement with the simulated ones. Stable broadside patterns with low cross polarization level are obtained for the three polarization modes. From Fig. 10 and 11, it can be observed that the proposed antenna has good CP radiation performance for the two CP modes. For the LP mode, the measured cross-polarization levels at both E- and H-plane are lower than -20 dB, as shown in Fig. 12.

All the simulated and measured results presented above show that the proposed patch antenna can work with three polarization modes at eight discrete operating frequency bands, and has good performance for all the operating modes. On the one hand, the directivity of the antenna with a fixed aperture keeps increasing as the frequency increases. On the other hand, the efficiency of the most reported frequency reconfigurable antennas also increases as the operating frequency goes up and has a big fluctuation within the whole frequency band. As a result, the realized gain has a big change within the whole frequency band. In this work, by utilizing the loss-character of p-i-n diodes, the variation tendency of the efficiency is just the opposite that of the directivity, which results in a stable realized gain within the whole operating frequency band. Finally, the performance of some up-to-date frequency and polarization reconfigurable antennas and this work is summarized in Table 3 for comparison. It shows that the proposed antenna has a high efficiency, a wide switching frequency range, and a good element gain with a relatively small variation less than 1.8 dB across all the operating states.

IV. CONCLUSION

To conclude, a reconfigurable patch antenna combined frequency agility and polarization diversity has been designed and implemented in this paper. By properly switching shorting pins, the operating frequency can be dynamically selected from eight discrete frequency bands due to the shunt inductive effect of the shorting pins. Simultaneously, the polarization can be independently reconfigured among three states, i.e., LHCP, RHCP and LP, by controlling the states of perturbation segments. The simulated and measured results are in good agreement. The proposed patch antenna has the advantages of simple reconfigurable network, a wide switching frequency range, a good element gain, and a small gain variation

across all the operating modes. It can be potentially used for advanced wireless communication systems.

REFERENCES

[1] L. Ge and K.-M. Luk, "A band-reconfigurable antenna based on directed dipole," *IEEE Trans. Antennas Propag.*, vol. 62, no. 1, pp. 64–71, Jan. 2014.

[2] H. L. Zhu, X. H. Liu, S. W. Cheung, and T. I. Yuk, "Frequency-reconfigurable antenna using metasurface," *IEEE Trans. Antennas Propag.*, vol. 62, no. 1, pp. 80–85, Jan. 2014.

[3] M. Gholamrezaei, F. Geran, and R. A. Sadeghzadeh, "Completely independent multi-ultrawideband and multi-dual-band frequency reconfigurable annular sector slot antenna (FR-ASSA)," *IEEE Trans. Antennas Propag.*, vol. 65, no. 2, pp. 893–898, Feb. 2017.

[4] M. S. Alam and A. M. Abbosh, "Beam-steerable planar antenna using circular disc and four pin-controlled tapered stubs for WiMAX and WLAN applications," *IEEE Antennas Wireless Propag. Lett.*, vol. 15, pp. 980–983, 2016.

[5] L. Ge and K. M. Luk, "Beamwidth reconfigurable magneto-electric dipole antenna based on tunable strip grating reflector," *IEEE Access*, vol. 4, pp. 7039–7045, 2016.

[6] M. S. Alam and A. M. Abbosh, "Wideband pattern-reconfigurable antenna using pair of radial radiators on truncated ground with switchable director and reflector," *IEEE Antennas Wireless Propag. Lett.*, vol. 16, pp. 24–28, 2017.

[7] Z.-C. Hao, H.-H. Wang, and W. Hong, "A novel planar reconfigurable monopulse antenna for indoor smart wireless access points' application," *IEEE Trans. Antenna Propag.*, vol. 64, no. 4, pp. 1250–1261, Apr. 2016.

[8] L. Chang, Y. Li, Z. Zhang, and Z. Feng, "Reconfigurable 2-bit fixed-frequency beam steering array based on microstrip line," *IEEE Trans. Antenna Propag.*, vol. 66, no. 2, pp. 683–691, Feb. 2018.

[9] Y. Yang, R. B. V. B. Simorangkir, X. Zhu, K. Esselle, and Q. Xue, "A novel boresight and conical pattern reconfigurable antenna with the diversity of 360ř polarization scanning," *IEEE Trans. Antenna Propag.*, vol. 65, no. 11, pp. 5747–5756, Nov. 2017.

[10] W. Lin, H. Wong, and R. W. Ziolkowski, "Wideband pattern-reconfigurable antenna with switchable broadside and conical beams," *IEEE Antennas Wireless Propag. Lett.*, vol. 16, pp. 2638–2641, 2017.

[11] S. Xiao, C. Zheng, M. Li, J. Xiong, and B.-Z. Wang, "Varactor-loaded pattern reconfigurable array for wide-angle scanning with low gain fluctuation," *IEEE Trans. Antennas Propag.*, vol. 63, no. 5, pp. 2364–2369, May 2015.

[12] Y. Li, Z. Zhang, J. Zheng, Z. Feng, and M. F. Iskander, "Experimental analysis of a wideband pattern diversity antenna with compact reconfigurable CPW-to-slotline transition feed," *IEEE Trans. Antennas Propag.*, vol. 59, no. 11, pp. 4222–4228, Nov. 2011.

[13] Y. Cao, S. W. Cheung, and T. I. Yuk, "A simple planar polarization reconfigurable monopole antenna for GNSS/PCS," *IEEE Trans. Antennas Propag.*, vol. 63, no. 2, pp. 500–507, Feb. 2015.

[14] J. Hu, Z.-C. Hao, and W. Hong, "Design of a wideband quad-polarization reconfigurable patch antenna array using a stacked structure," *IEEE Trans. Antenna Propag.*, vol. 65, no. 6, pp. 3014–3023, Jun. 2017.

[15] S.-L. Chen, P.-Y. Qin, C. Ding, and Y. J. Guo, "Cavity-backed proximity-coupled reconfigurable microstrip antenna with agile polarizations and steerable beams," *IEEE Trans. Antennas Propag.*, vol. 65, no. 10, pp. 5553–5558, Oct. 2017.

[16] W. Lin and H. Wong, "Wideband circular-polarization reconfigurable antenna with L-shaped feeding probes," *IEEE Antennas Wireless Propag. Lett.*, vol. 16, pp. 2114–2117, 2017.

[17] Z. Hu, S. Wang, Z. Shen, and W. Wu, "Broadband polarization-reconfigurable water spiral antenna of low profile," *IEEE Antennas Wireless Propag. Lett.*, vol. 16, pp. 1377–1380, 2017.

[18] Z.-C. Hao, K.-K. Fan, and H. Wang, "A planar polarization-reconfigurable antenna," *IEEE Trans. Antennas Propag.*, vol. 65, no. 4, pp. 1624–1632, Apr. 2017.

[19] J. Hu, Z. C. Hao, and Z. W. Miao, "Design and implementation of a planar polarization-reconfigurable antenna," *IEEE Antennas Wireless Propag. Lett.*, vol. 16, pp. 1557–1560, 2017.

[20] F. Wu and K. M. Luk, "Single-port reconfigurable magneto-electric dipole antenna with quad-polarization diversity," *IEEE Trans. Antennas Propag.*, vol. 65, no. 5, pp. 2289–2296, May 2017.

[21] Y. Li, Z. Zhang, W. Chen, and Z. Feng, "Polarization reconfigurable slot antenna with a novel compact CPW-to-slotline transition for WLAN application," *IEEE Antennas Wireless Propag. Lett.*, vol. 9, pp. 252–255, 2010.

[22] C. Huang, W. Pan, X. Ma, B. Zhao, J. Cui, and X. Luo, "Using reconfigurable transmitarray to achieve beam-steering and polarization manipulation applications," *IEEE Trans. Antennas Propag.*, vol. 63, no. 11, pp. 4801–4810, Nov. 2015.

[23] P. K. Li, Z. H. Shao, Q. Wang, and Y. J. Cheng, "Frequency- and pattern-reconfigurable antenna for multistandard wireless applications," *IEEE Antennas Wireless Propag. Lett.*, vol. 14, pp. 333–336, 2015.

[24] D. Rodrigo, B. A. Cetiner, and L. Jofre, "Frequency, radiation pattern and polarization reconfigurable antenna using a parasitic pixel layer," *IEEE Trans. Antennas Propag.*, vol. 62, no. 6, pp. 3422–3427, Jun. 2014.

[25] L. Ge, Y. Li, J. Wang, and C.-Y.-D. Sim, "A low-profile reconfigurable cavity-backed slot antenna with frequency, polarization, and radiation pattern agility," *IEEE Trans. Antennas Propag.*, vol. 65, no. 5, pp. 2182–2189, May 2017.

[26] B. Babakhani, S. K. Sharma, and N. R. Labadie, "A frequency agile microstrip patch phased array antenna with polarization reconfiguration," *IEEE Trans. Antennas Propag.*, vol. 64, no. 10, pp. 4316–4327, Oct. 2016.

[27] J.-S. Row and C.-J. Shih, "Polarization-diversity ring slot antenna with frequency agility," *IEEE Trans. Antennas Propag.*, vol. 60, no. 8, pp. 3953–3957, Aug. 2012.

[28] N. Nguyen-Trong, A. Piotrowski, L. Hall, and C. Fumeaux, "A frequency- and polarization-reconfigurable circular cavity antenna," *IEEE Antennas Wireless Propag. Lett.*, vol. 16, pp. 999–1002, 2017.

[29] B. Liang, B. Sanz-Izquierdo, E. A. Parker, and J. C. Batchelor, "A frequency and polarization reconfigurable circularly polarized antenna using active EBG structure for satellite navigation," *IEEE Trans. Antennas Propag.*, vol. 63, no. 1, pp. 33–40, Jan. 2015.

[30] K. M.-J. Ho and G. M. Rebeiz, "A 0.9–1.5 GHz microstrip antenna with full polarization diversity and frequency agility," *IEEE Trans. Antenna Propag.*, vol. 62, no. 5, pp. 2398–2406, May 2014.

[31] M. Wang, M. R. Khan, M. D. Dickey, and J. J. Adams, "A compound frequency- and polarization- reconfigurable crossed dipole using multidirectional spreading of liquid metal," *IEEE Antennas Wireless Propag. Lett.*, vol. 16, pp. 79–82, 2017.

[32] P.-Y. Qin, Y. J. Guo, Y. Cai, E. Dutkiewicz, and C.-H. Liang, "A reconfigurable antenna with frequency and polarization agility," *IEEE Antennas Wireless Propag. Lett.*, vol. 10, pp. 1373–1376, Dec. 2011.

[33] N. Nguyen-Trong, L. Hall, and C. Fumeaux, "A frequency- and polarization-reconfigurable stub-Loaded microstrip patch antenna," *IEEE Trans. Antennas Propag.*, vol. 63, no. 11, pp. 5235–5240, Nov. 2015.

[34] L.-R. Tan, R.-X. Wu, and Y. Poo, "Magnetically reconfigurable SIW antenna with tunable frequencies and polarizations," *IEEE Trans. Antenna Propag.*, vol. 63, no. 6, pp. 2772–2776, Jun. 2015.

[35] D. Schaubert, F. Farrar, A. Sindoris, and S. Hayes, "Microstrip antennas with frequency agility and polarization diversity," *IEEE Trans. Antennas Propag.*, vol. AP-29, no. 1, pp. 118–123, Jan. 1981.

[36] J. Hu and Z. C. Hao, "Frequency and polarization reconfigurable patch antenna using switchable shorting pins," in *Proc. IEEE 7th Asia–Pacific Conf. Antennas Propag. (APCAP)*, Auckland, New Zealand, Aug. 2018, pp. 1–2.

[37] X. Zhang and L. Zhu, "Gain-enhanced patch antennas with loading of shorting pins," *IEEE Trans. Antennas Propag.*, vol. 64, no. 8, pp. 3310–3318, Aug. 2016.

[38] X. Zhang and L. Zhu, "Gain-enhanced patch antenna without enlarged size via loading of slot and shorting pins," *IEEE Trans. Antennas Propag.*, vol. 65, no. 11, pp. 5702–5709, Nov. 2017.

[39] X. Zhang and L. Zhu, "High-gain circularly polarized microstrip patch antenna with loading of shorting pins," *IEEE Trans. Antennas Propag.*, vol. 64, no. 6, pp. 2172–2178, Jun. 2016.

[40] X. Zhang, L. Zhu, and N.-W. Liu, "Pin-loaded circularly-polarized patch antennas with wide 3-dB axial ratio beamwidth," *IEEE Trans. Antennas Propag.*, vol. 65, no. 2, pp. 521–528, Feb. 2017.

[41] MACOM Company. *MADP-000907-14020P PIN Diode*. Accessed: 2015. [Online]. Available: http://www.macom.com/products/product-detail/MADP-000907-14020P

[42] B. Y. Toh, R. Cahill, and V. F. Fusco, "Understanding and measuring circular polarization," *IEEE Trans. Edu.*, vol. 46, no. 3, pp. 313–318, Aug. 2003.

[43] Z.-C. Hao, X. Liu, X. Huo, and K.-K. Fan, "Planar high-gain circularly polarized element antenna for array applications," *IEEE Trans. Antenna Propag.*, vol. 63, no. 5, pp. 1937–1948, May 2015.
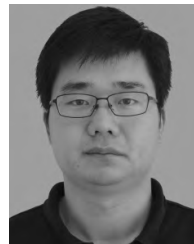
JUN HU (S'17) received the B.S. degree in electronics and information engineering from Anhui Agricultural University, Hefei, China, in 2012, and the M.S. degree in electromagnetic field and microwave technology from Southeast University, Nanjing, China, in 2014, where he is currently pursuing the Ph.D. degree in electronic science and technology.

His recent research interests include the design of tunable devices, passive components, reconfigurable antennas, and antenna array.

ZHANG-CHENG HAO (M'08–SM'15) received the B.S. degree in microwave engineering from Xidian University, Xi'an, China, in 1997, and the M.S. and Ph.D. degrees in radio engineering from Southeast University, Nanjing, China, in 2002 and 2006, respectively. In 2006, he was a Post-Doctoral Researcher with the Laboratory of Electronics and Systems for Telecommunications, École Nationale Supérieure des Télécommunications de Bretagne, Bretagne, France, where he was involved in developing millimeter-wave antennas. In 2007, he joined the Department of Electrical, Electronic and Computer Engineering, Heriot-Watt University, Edinburgh, U.K., as a Research Associate, where he was involved in developing multilayer integrated circuits and ultra-wide-band components. In 2011, he joined the School of Information Science and Engineering, Southeast University, as a Professor. He has authored or co-authored over 150 referred journal and conference papers. He holds 20 granted patents. His current research interests involve microwave and millimeter-wave systems, submillimeter-wave and terahertz components, and passive circuits, including filters, antenna arrays, couplers, and multiplexers.

Dr. Hao has served as a Reviewer for many technique journals, including the Ieee Transactions Microwave Theory and Techniques, the Ieee Transactions on Antennas and Propagation, *the* IEEE AWPL, and *the* IEEE MWCL. He was a recipient of the Thousands of Young Talents from the China Government in 2011 and the High Level Innovative and Entrepreneurial Talent by Jiangsu Province, China, in 2012.

• • •